Henry Rossiter
Daniel Fonseka
Braden Conrad
Gareth Meredith

# OpenFOAM Assignment 1

## Non-Dimensional Continuity and Momentum

$$\tilde{x} = \frac{x}{L}, \tilde{y} = \frac{y}{L}$$
$$\tilde{u} = \frac{u}{U}, \tilde{x} = \frac{v}{U}$$
$$\tilde{\rho} = \frac{\rho}{\rho U^2}, \tilde{t} = t\frac{U}{L}$$

**Continuity:**

$$\frac{\mathrm{d}u}{\mathrm{d}x} + \frac{\mathrm{d}v}{\mathrm{d}y} = 0$$
$$\frac{\mathrm{d}\tilde{u}U}{\mathrm{d}\tilde{x}L} + \frac{\mathrm{d}\tilde{v}U}{\mathrm{d}\tilde{y}L} = 0$$
$$\boxed{\frac{U}{L}[\frac{\mathrm{d}\tilde{u}}{\mathrm{d}\tilde{x}} + \frac{\mathrm{d}\tilde{v}}{\mathrm{d}\tilde{y}}] = 0}$$

**Momentum:**
**x:**

$$\rho[\frac{\mathrm{d}u}{\mathrm{d}t} + u\frac{\mathrm{d}u}{\mathrm{d}x} + v\frac{\mathrm{d}u}{\mathrm{d}y}] = -\frac{\mathrm{d}\rho}{\mathrm{d}x} + \mu[\frac{\mathrm{d}^2u}{\mathrm{d}x^2} + \frac{\mathrm{d}^2v}{\mathrm{d}y^2}]$$

$$\rho[\frac{\mathrm{d}(\tilde{u}U)}{\mathrm{d}(\tilde{t}\frac{L}{U})} + \tilde{u}U\frac{\mathrm{d}(\tilde{u}U)}{\mathrm{d}(\tilde{x}L)} + \tilde{v}U\frac{\mathrm{d}(\tilde{u}U)}{\mathrm{d}(\tilde{y}L)}] = -\frac{\mathrm{d}(\tilde{\rho}\rho U^2)}{\mathrm{d}(\tilde{x}L)} + \mu[\frac{\mathrm{d}^2(\tilde{u}U)}{\mathrm{d}(\tilde{x}L)^2} + \frac{\mathrm{d}^2(\tilde{v}U)}{\mathrm{d}(\tilde{y}L)^2}]$$

$$\frac{\rho U^2}{L}[\frac{\mathrm{d}\tilde{u}}{\mathrm{d}\tilde{t}} + \tilde{u}\frac{\mathrm{d}\tilde{u}}{\mathrm{d}\tilde{x}} + v\frac{\mathrm{d}\tilde{u}}{\mathrm{d}\tilde{y}}] = -\frac{\rho U^2}{L}\frac{\mathrm{d}\tilde{\rho}}{\mathrm{d}\tilde{x}} + \frac{\mu U}{L^2}[\frac{\mathrm{d}^2\tilde{u}}{\mathrm{d}\tilde{x}^2} + \frac{\mathrm{d}^2\tilde{v}}{\mathrm{d}\tilde{y}^2}]$$

$$\boxed{\frac{\mathrm{d}\tilde{u}}{\mathrm{d}\tilde{t}} + \tilde{u}\frac{\mathrm{d}\tilde{u}}{\mathrm{d}\tilde{x}} + v\frac{\mathrm{d}\tilde{u}}{\mathrm{d}\tilde{y}} = -\frac{\mathrm{d}\tilde{\rho}}{\mathrm{d}\tilde{x}} + \frac{\mu}{\rho UL}[\frac{\mathrm{d}^2\tilde{u}}{\mathrm{d}\tilde{x}^2} + \frac{\mathrm{d}^2\tilde{v}}{\mathrm{d}\tilde{y}^2}]}$$

similarly,
**y:**

$$\boxed{\frac{\mathrm{d}\tilde{v}}{\mathrm{d}\tilde{t}} + \tilde{u}\frac{\mathrm{d}\tilde{v}}{\mathrm{d}\tilde{x}} + v\frac{\mathrm{d}\tilde{v}}{\mathrm{d}\tilde{y}} = -\frac{\mathrm{d}\tilde{\rho}}{\mathrm{d}\tilde{y}} + \frac{\mu}{\rho UL}[\frac{\mathrm{d}^2\tilde{u}}{\mathrm{d}\tilde{x}^2} + \frac{\mathrm{d}^2\tilde{v}}{\mathrm{d}\tilde{y}^2}]}$$

$$\frac{\mu}{\rho UL} = \frac{1}{Re} \text{ (where Re is Reynold's number)}$$

- As $\mathrm{Re} \to \infty$, the viscous term approaches 0, because $\frac{\mu}{\rho UL}$ approaches 0, and becomes less influential on system behavior.

- As $\mathrm{Re} \to 0$, $\frac{\mu}{\rho UL} \to \infty$, so the viscous term becomes more influential on the behavior of the system.

**Description of the flow for Re = 10**

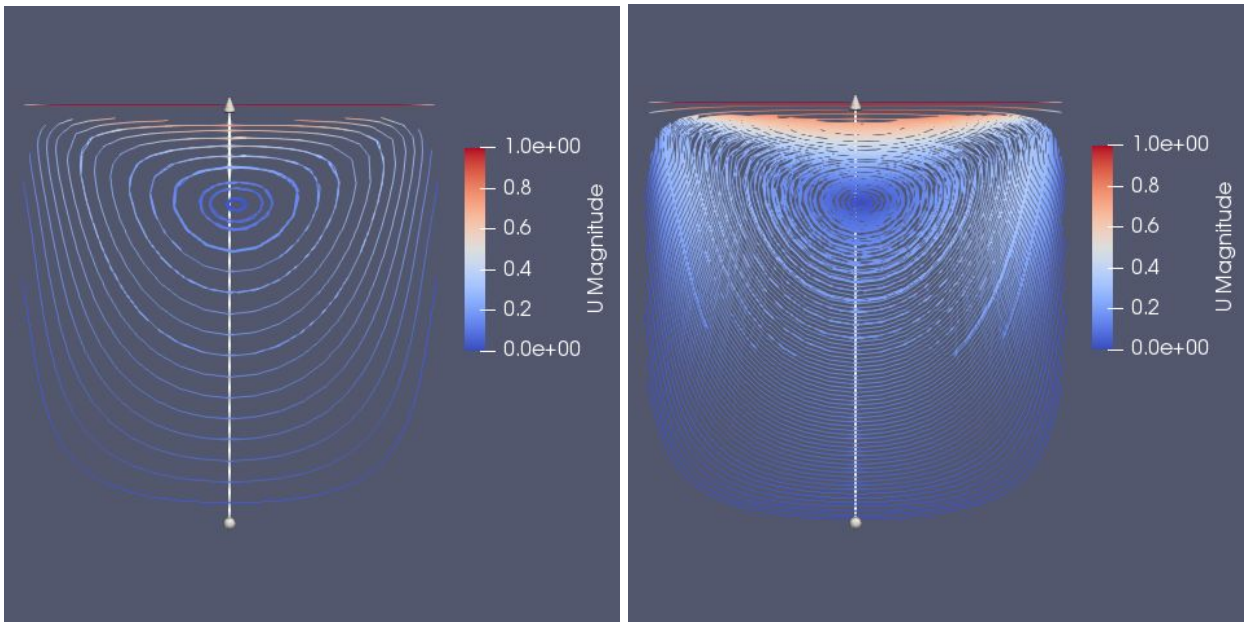


**Figure 1.** Two-dimensional contour plots of velocity within the cavity. Figures generated with ParaView's stream function filter with resolutions of 20 (left) and 100 (right). Simulation was run from $t = 0$ to $t = 0.5$ with a $20 \times 20$ mesh and a time step of $\Delta t = 0.005$.

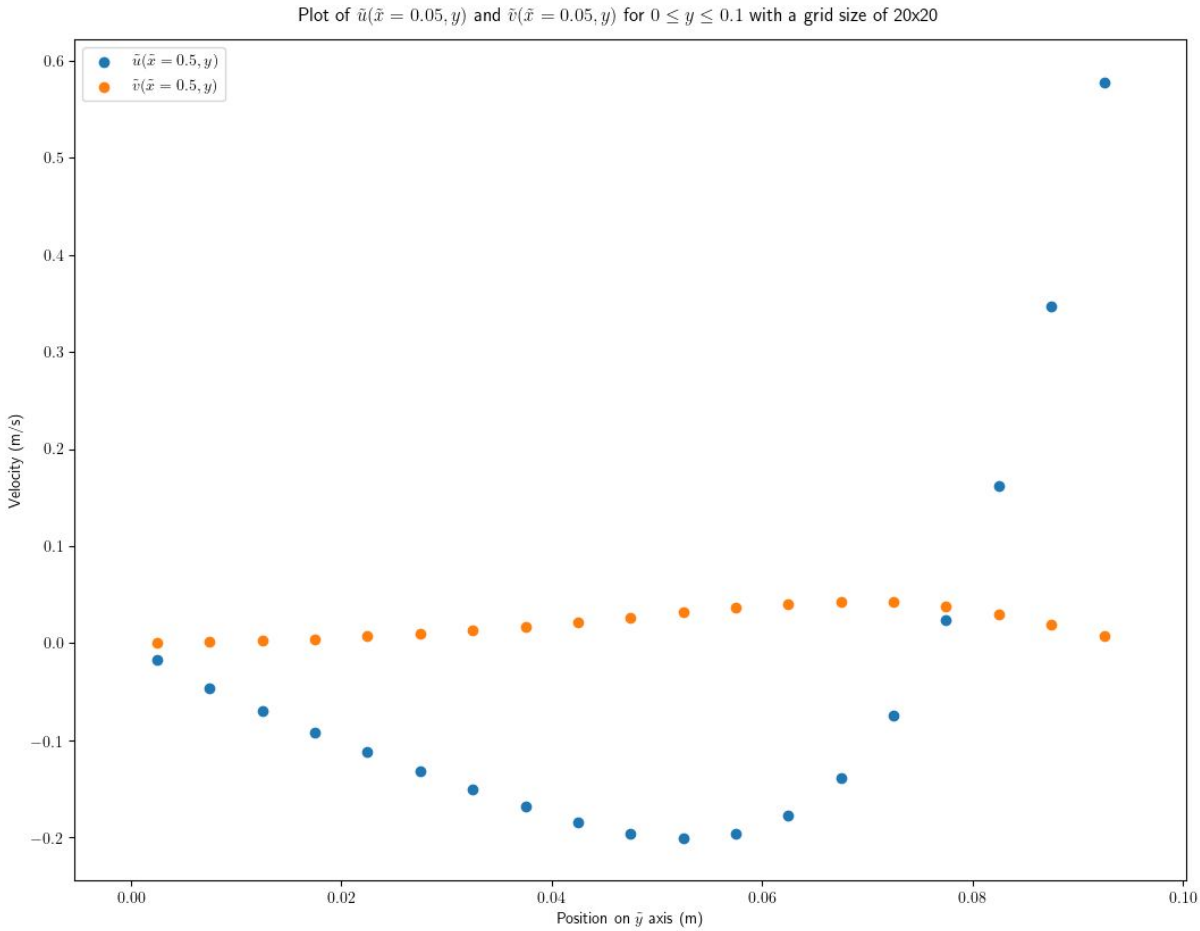


**Figure 2**. Plot of velocity components along the direction y through the center of the cavity. Simulation was run from $t = 0$ to $t = 0.5$ with a $20 \times 20$ mesh and a timestep of $\Delta t = 0.005$.

**Refining the Solution**

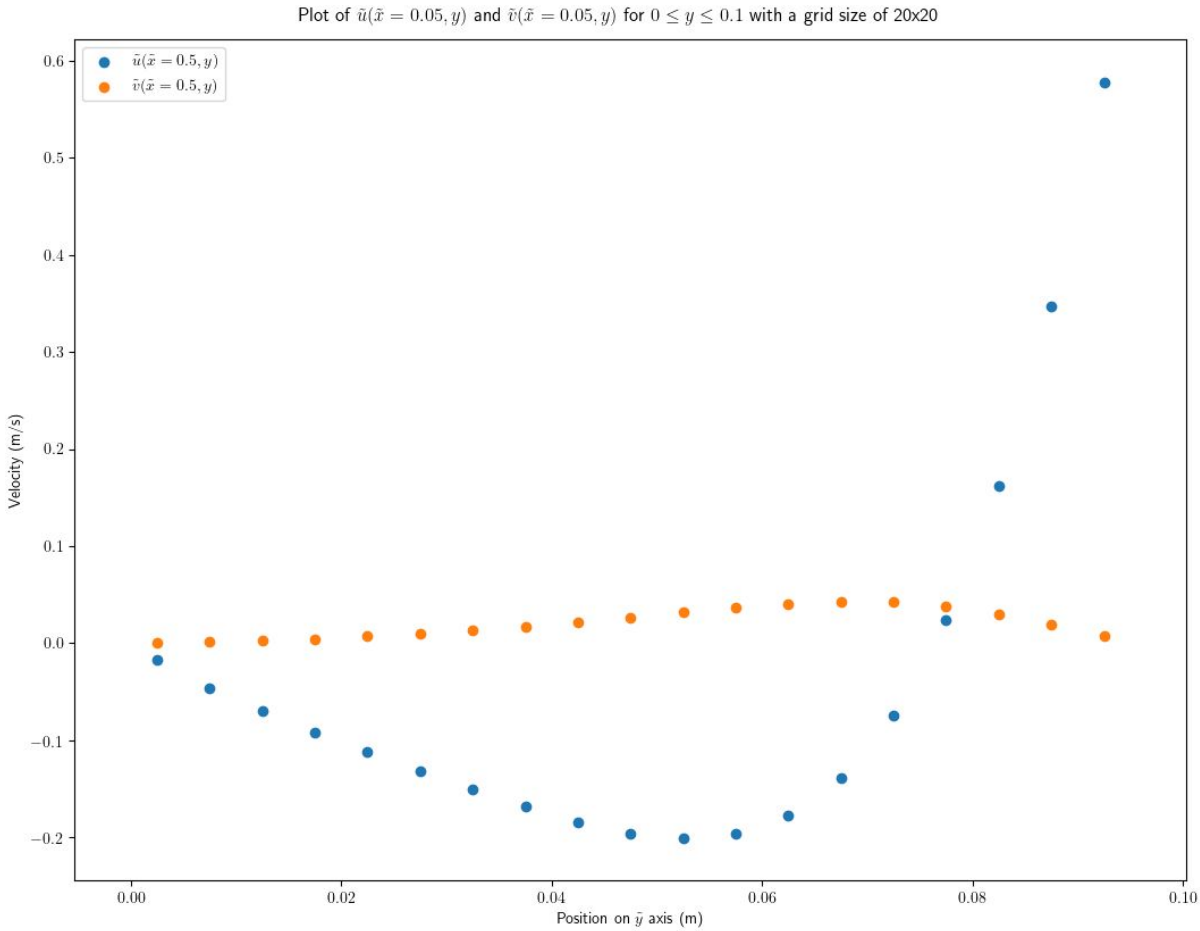


**Figure 3**. Plot of velocity components along the direction y through the center of the cavity. Simulation was run from $t = 0$ to $t = 0.5$ with a $20 \times 20$ mesh and a timestep of $\Delta t = 0.005$.

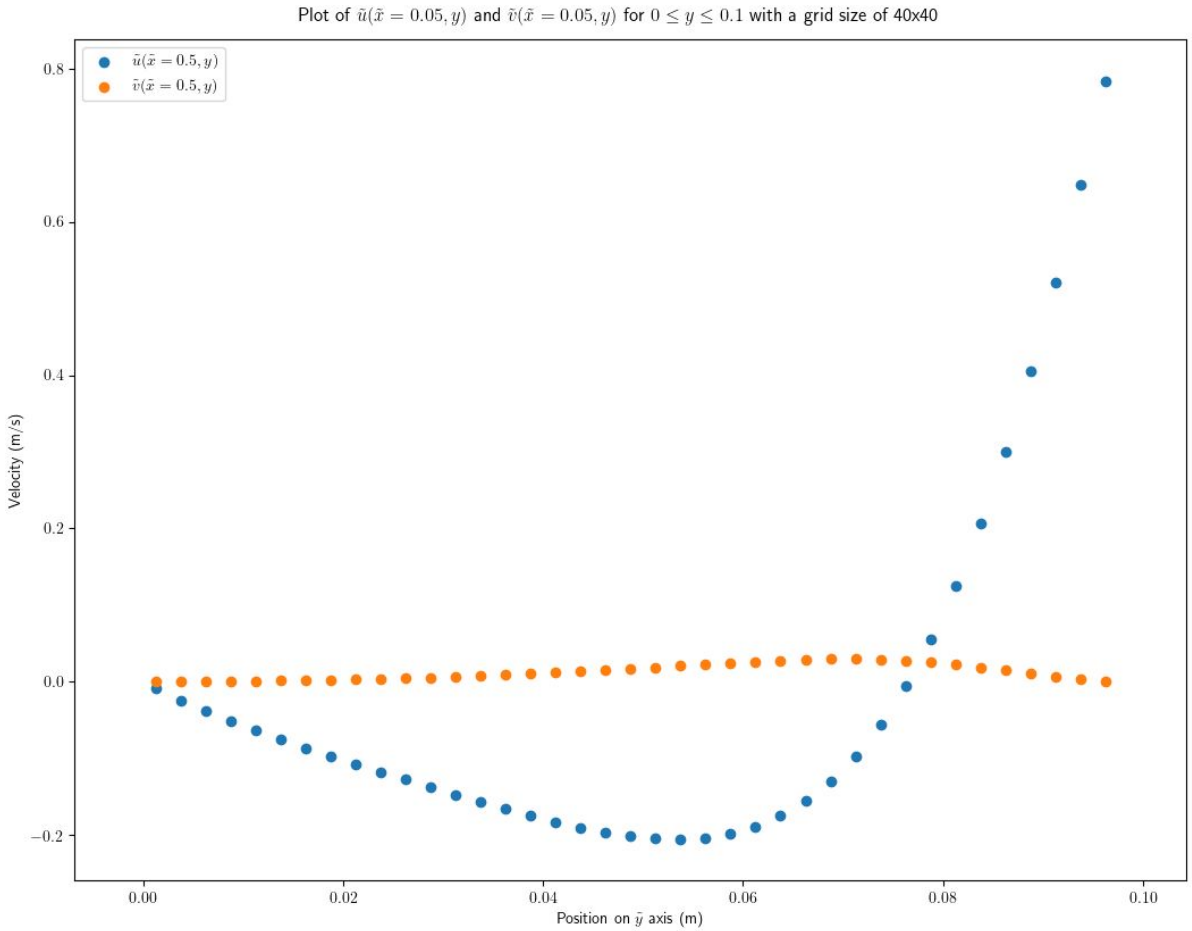


**Figure 4**. Plot of velocity components along the direction y through the center of the cavity. Simulation was run from $t = 0$ to $t = 0.5$ with a $40 \times 40$ mesh and a timestep of $\Delta t = 0.0025$.

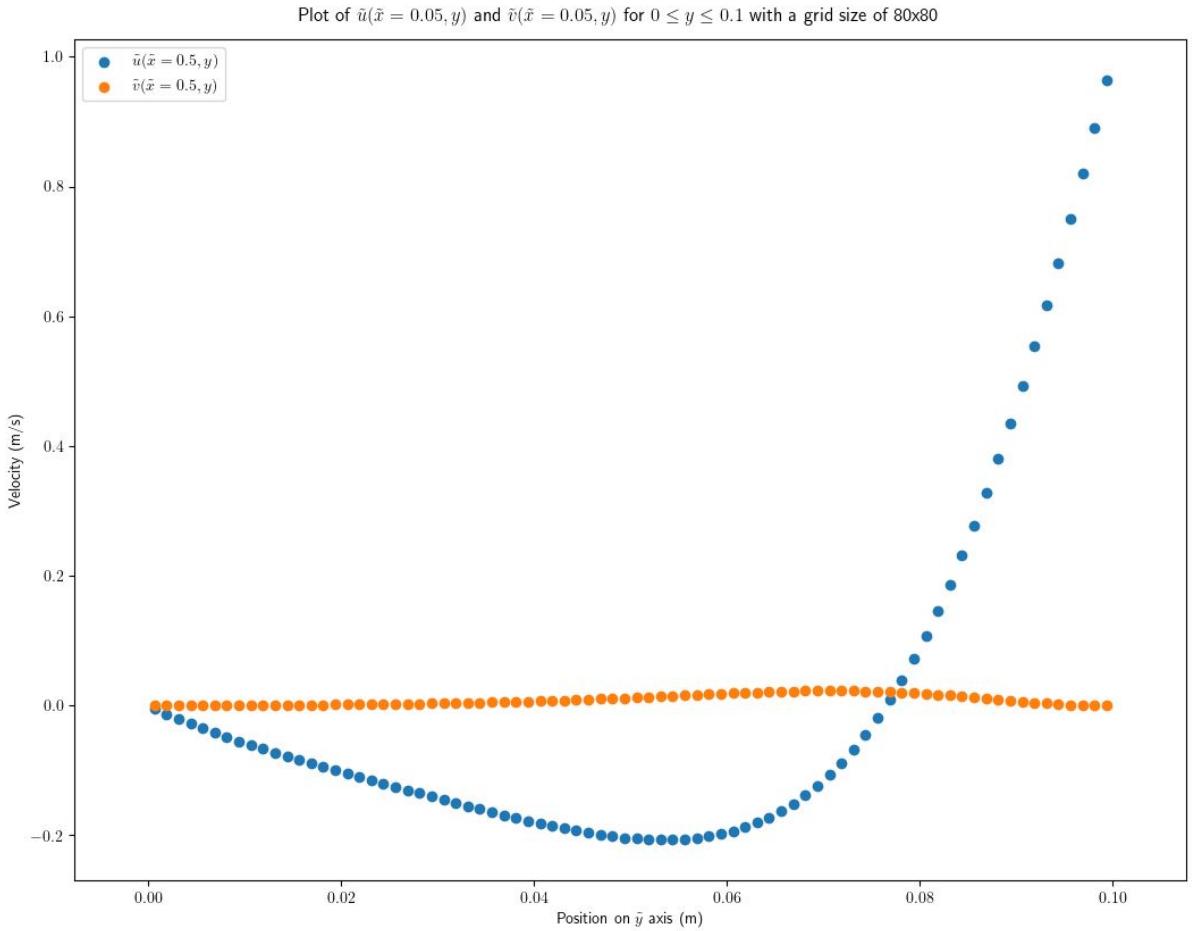


**Figure 5**. Plot of velocity components along the direction y through the center of the cavity. Simulation was run from $t = 0$ to $t = 0.5$ with a $80 \times 80$ mesh and a timestep of $\Delta t = 0.00125$.

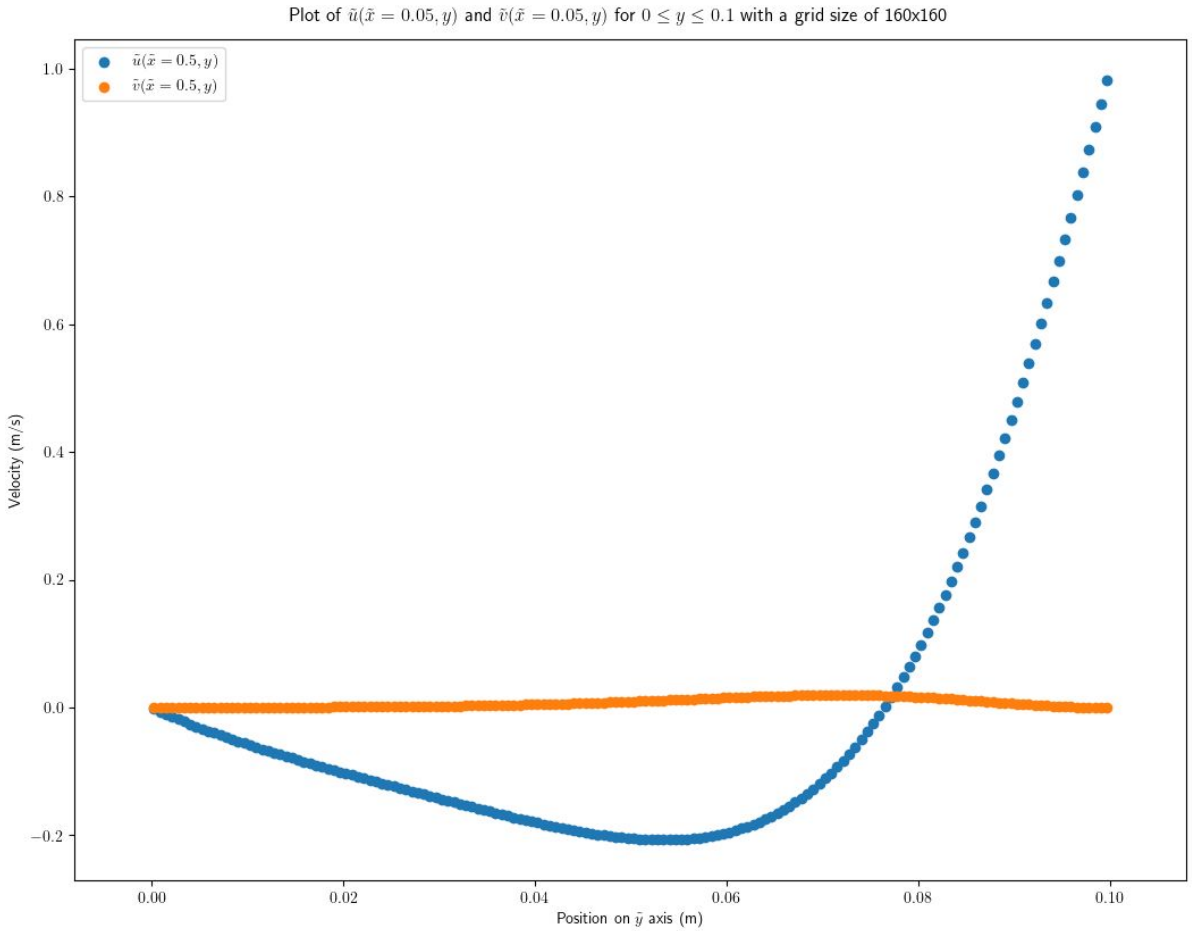


**Figure 6**. Plot of velocity components along the direction y through the center of the cavity. Simulation was run from $t = 0$ to $t = 0.5$ with a $160 \times 160$ mesh and a timestep of $\Delta t = 0.000625$.

From an examination of the above four plots, one can see the development of a CFD solution as grid size and timestep are altered. **Figure 3** shows the solution for both velocity components with a grid size of $20 \times 20$ and a time step of 0.005 seconds. In each proceeding plot, the timestep is halved and the grid size is doubled. One can clearly see the effect of decreasing the step size, there is simply more solution data points generated when step size is smaller. This is why **Figure 3** with a 0.005s time step displays far fewer data points than **Figure 7** with a 0.000625s time step. Although the effect of altering the grid size is less obvious, it is perhaps even more important to an accurate solution. Most noticeably, **Figure 3**, with a $20 \times 20$ grid, does not appear to collect the full range of u~ velocity data, as it misses the high velocity portion that occurs around y=0.1. The highest velocity recorded in the solution by the $20 \times 20$ grid is around 0.6m/s, while the $160 \times 160$ grid captures velocity values of up to 1 m/s. Additionally, as the grid size is increased, the v~ solution appears to flatten out.

The wallclock time of each run is tabulated below. The wall clock time increases greatly as the total number of mesh points, *N*, is increased. Each simulation was conducted from $t = 0$ to $t = 0.5$, so the number of timesteps, *n*, can be calculated as $n = \frac{0.5}{\Delta t}$, where $\Delta t$ is the time step duration. For each trial we also calculated *C*, the wall clock time per time step.

| Mesh Points | | | Time Step Duration (s) | Number of Time Steps | Wall Clock Time (s) | C, Wall Clock Time per Time Step (s) |
|---|---|---|---|---|---|---|
| x | y | N, Total | | | | |
| 20 | 20 | 400 | 0.005 | 100 | 1.704 | 0.01704 |
| 40 | 40 | 1600 | 0.0025 | 200 | 5.217 | 0.026085 |
| 80 | 80 | 6400 | 0.00125 | 400 | 21.01 | 0.052525 |
| 160 | 160 | 25600 | 0.000625 | 800 | 224.815 | 0.281019 |

**Table 1**. Simulation wall clock times are measured for various mesh sizes. Output folders were cleared between simulations for consistency.

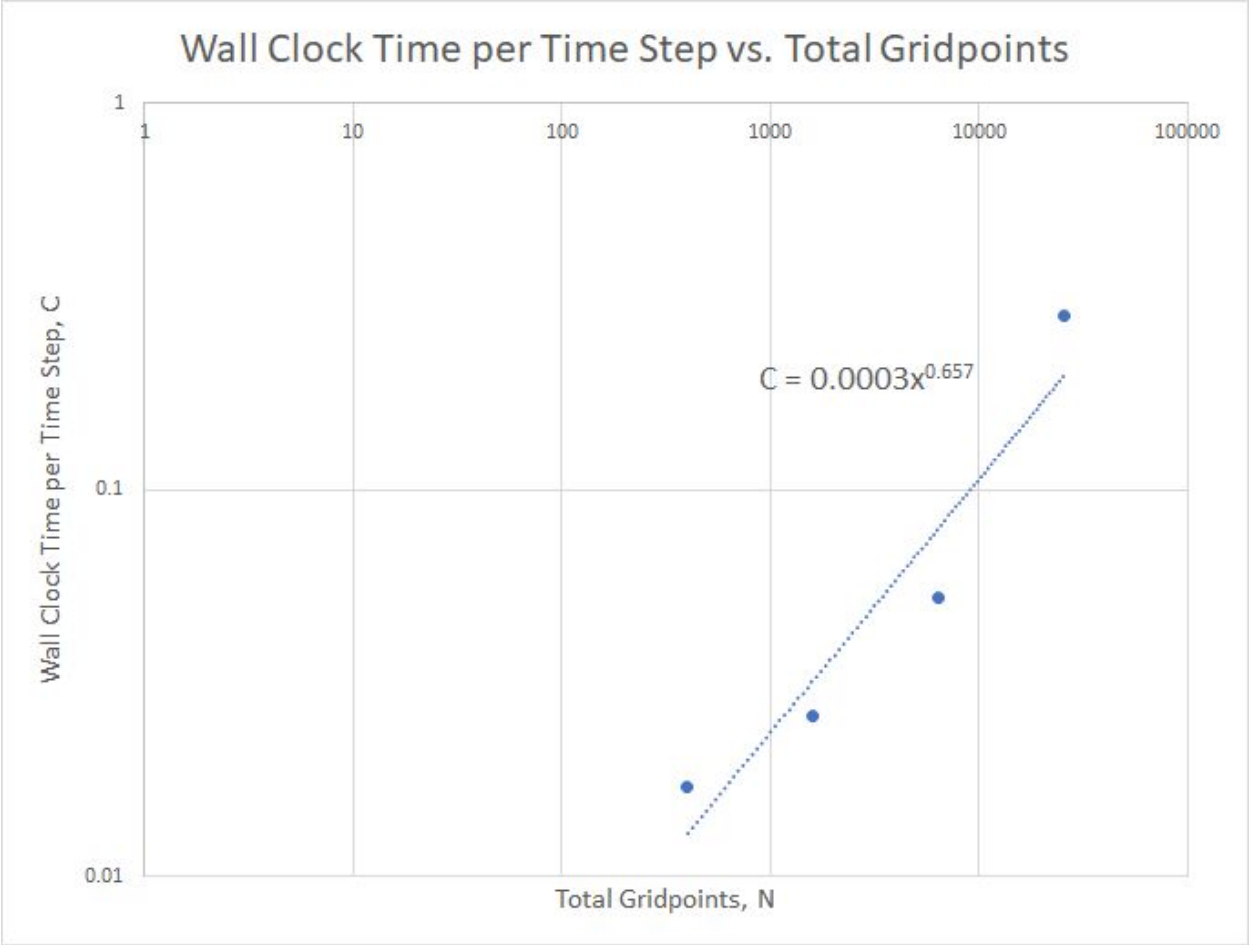


**Figure 7**. Log-Log plot of *C*, the wall clock time per time step, vs *N*, the total grid points. Line of best fit is overlaid.

**Figure 7** shows that *C* increases with the power of *N*. We fit our graph to the relationship

$$C = \beta N^{\alpha}$$

and obtained experimental values of $\beta = 0.0003$ and $\alpha = .657$.

**Force on the Lid**

Next, we investigated the stress, $\tau$, and force, $Fe$, along the surface of the lid. To approximate stress, $\tau$, along the lid we extracted data at points $x_i$ where $0 \le x_i \le 1$ at $y = 0.95$ and $y = 0.99$. Then, we used the one-sided finite difference approximation $\tau_i = \frac{u(x_i, y=0.99) - u(x_i, y=0.95)}{0.04}$ to obtain approximate values for $\tau_i$ at each point $x_i$, $y = 0.99$.

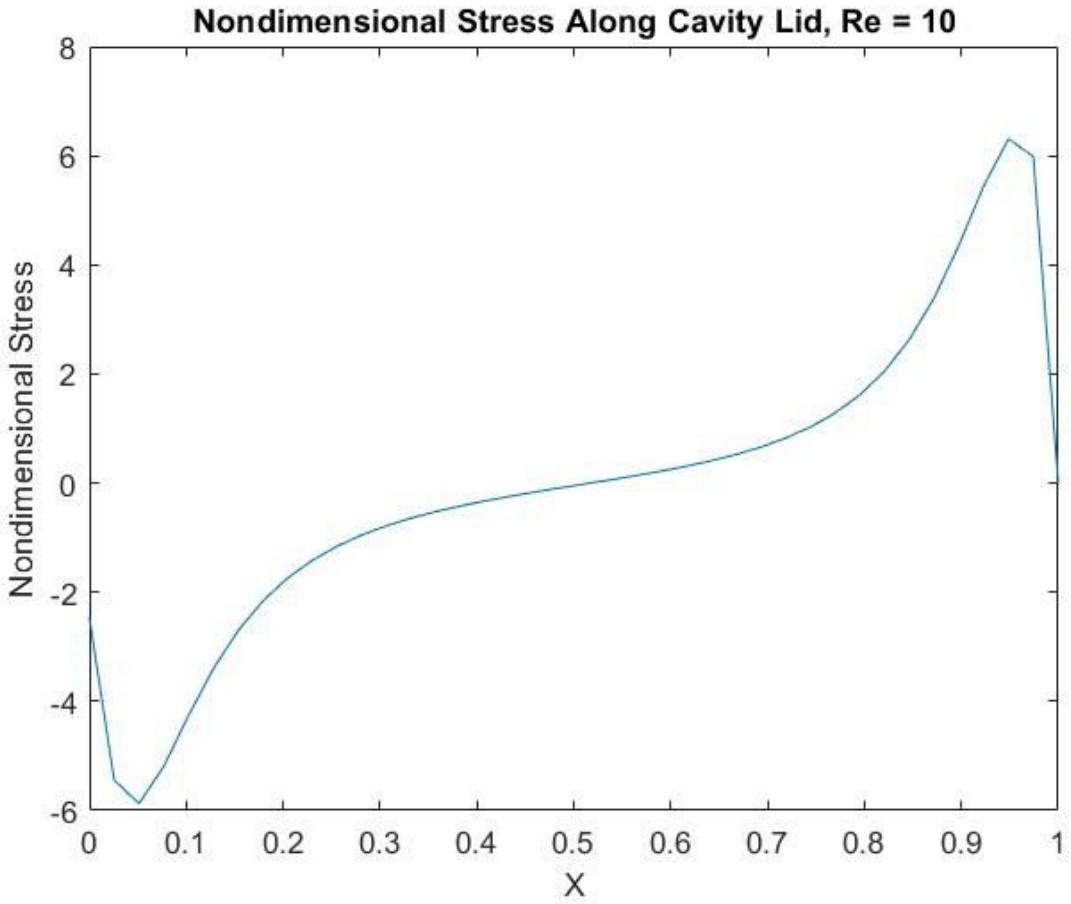


**Figure 8**. Non-dimensional stress along the lid of the cavity. Simulation was run with Re=10 from $t = 0$ to $t = 0.5$ with a $20 \times 20$ mesh and a timestep of $\Delta t = 0.005$.

Next, we executed simulations at Reynolds numbers between 10 and 500. Based on our results from the previous section, we used $40 \times 40$ mesh for these simulations.To manipulate Re, we altered viscosity, *v*, as shown in **Table 2** below.

| $U\ (m/s)$ | $L\ (m)$ | $v\ \ (m^2/s)$ | $Re$ |
|---|---|---|---|
| 1 | 0.1 | 0.01 | 10 |
| 1 | 0.1 | 0.002 | 50 |
| 1 | 0.1 | 0.001 | 100 |
| 1 | 0.1 | 0.0002 | 500 |

**Table 2**. Values used for $U$, $L$, and $v$ to achieve various Reynolds numbers.

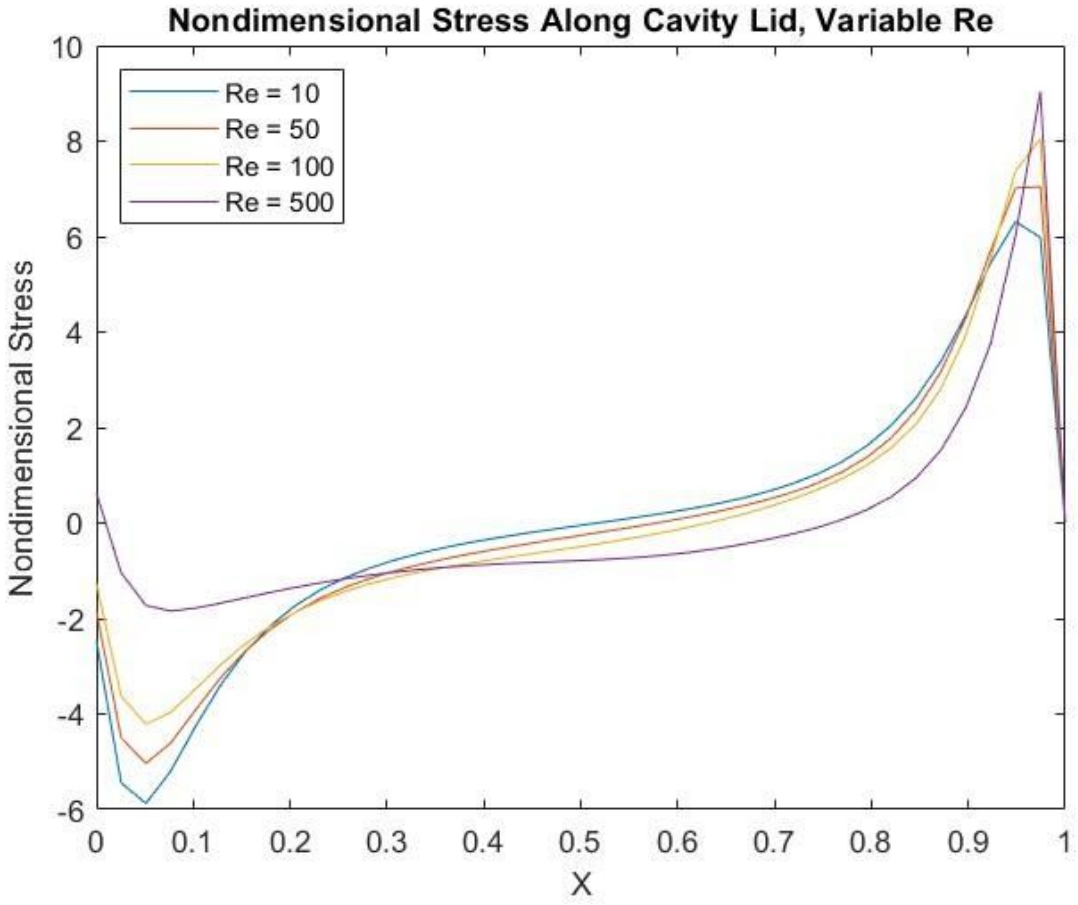


**Figure 9.** Plot showing non-dimensional stress on the cavity lid for varying values of Re. Simulations were run from $t = 0$ to $t = 0.5$ with a $40 \times 40$ mesh and a time step of $\Delta t = 0.005$.

Next, we calculated force, Fe, along the lid of the cavity. To calculate Fe, we used the trapezoidal rule to numerically integrate the non dimensional stress along the lid of the cavity. The effect of Re on force along the lid of the cavity is visualized in **Figure 10**. **Figure 10** indicates that simulations with lower Re values tend to induce lower forces on the lid.

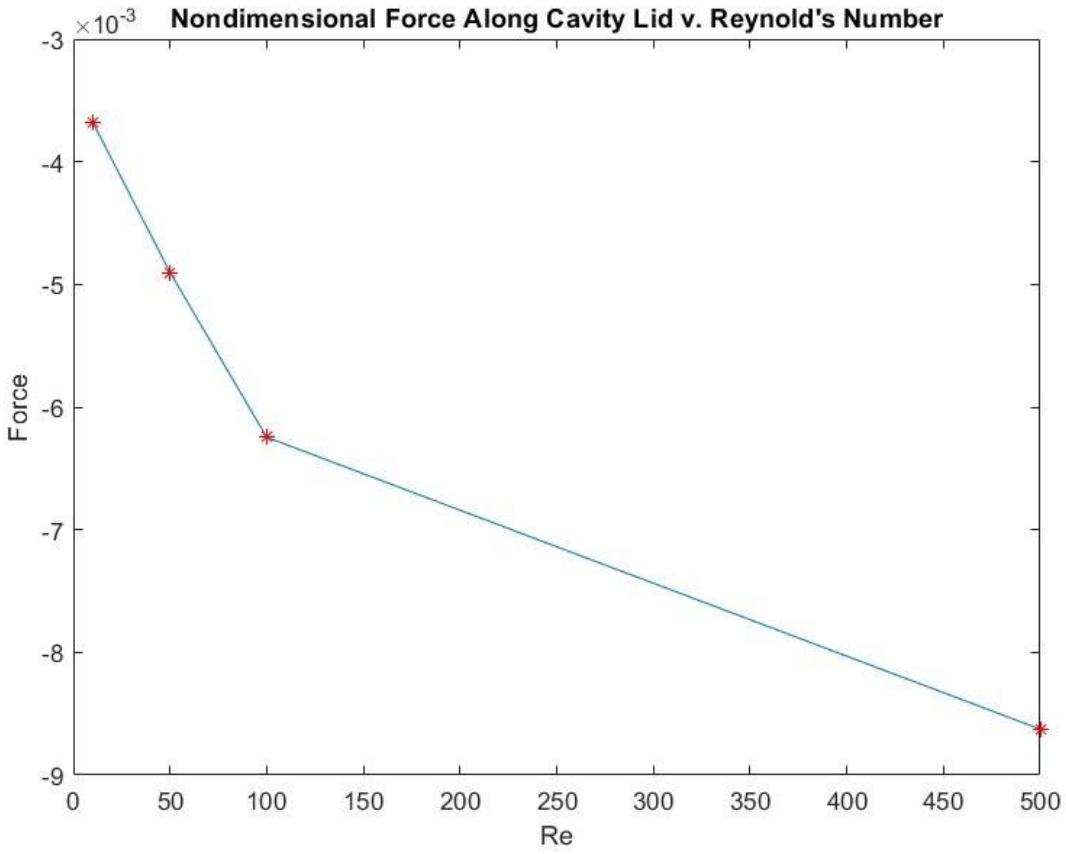


**Figure 10.** Graph that shows the non dimensional force Fe versus the Reynolds number. Reynolds number was calculated as $Re = \frac{UL}{v}$. Simulations were run from $t = 0$ to $t = 0.5$ with a $40 \times 40$ mesh and a time step of $\Delta t = 0.005$.

**Extra Credit**

Next, we executed simulations with altered cavity dimensions. We perform new simulations with H/L= 0.5, a shallow cavity, andH/L= 2, a tall cavity. For each pair of cavity dimensions, we executed trials with Reynolds numbers from 10 to 500. Simulation parameters are tabulated in **Table 3** below.

| **Dimensions** | | **Mesh Points** | | | |
|---|---|---|---|---|---|
| **L** | **H** | **x** | **y** | **H/L** | **Re** |
| 2 | 1 | 40 | 20 | 0.5 | 10 |
| 2 | 1 | 40 | 20 | 0.5 | 50 |
| 2 | 1 | 40 | 20 | 0.5 | 100 |

| | | | | | |
|---|---|---|---|---|---|
| 2 | 1 | 40 | 20 | 0.5 | 500 |
| 1 | 2 | 20 | 40 | 2 | 10 |
| 1 | 2 | 20 | 40 | 2 | 50 |
| 1 | 2 | 20 | 40 | 2 | 100 |
| 1 | 2 | 20 | 40 | 2 | 500 |

**Table 3**. Simulation parameters for trials with variable cavity dimensions and Reynolds numbers.

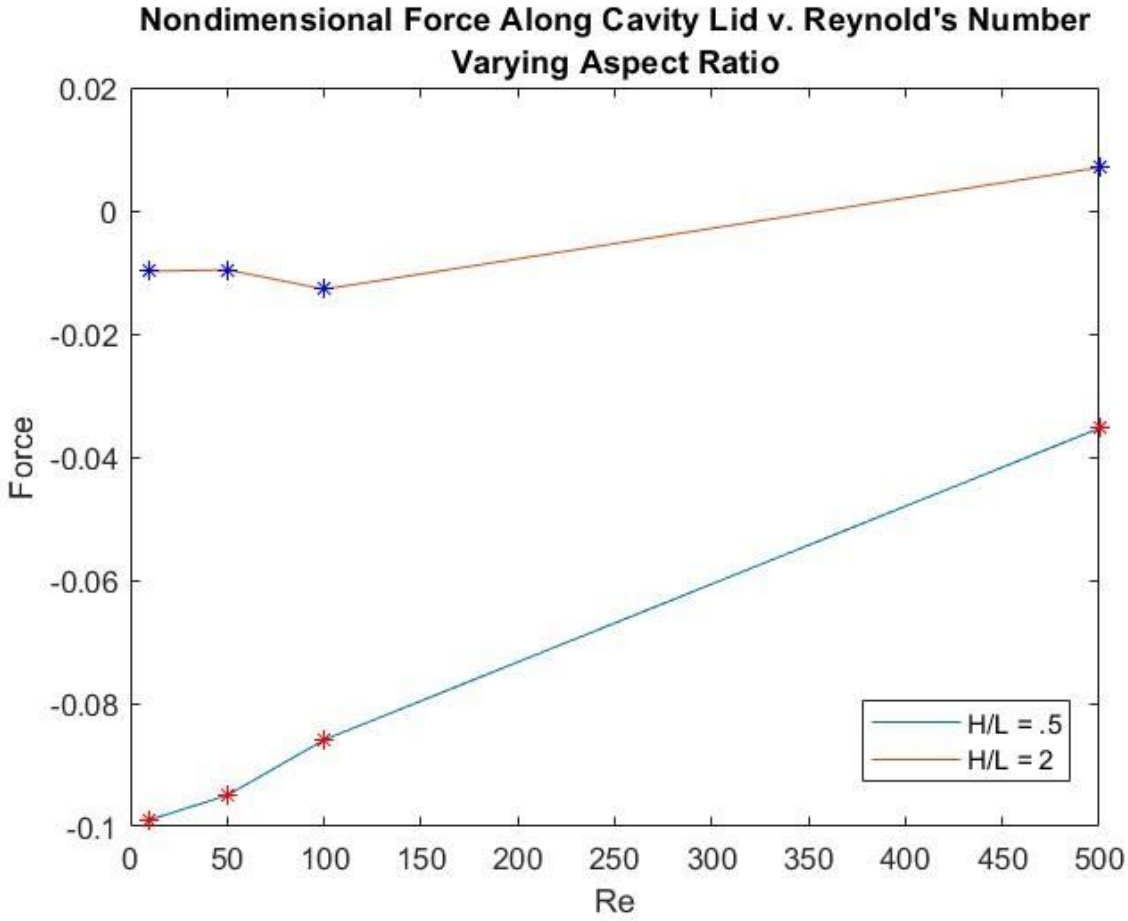


**Figure 11**. Graph that shows the non dimensional force Fe versus the Reynolds number for cavity dimensions of H/L=0.5 and H/L=2. Reynolds number was calculated as $Re = \frac{UL}{v}$. Simulations were run from $t = 0$ to $t = 0.5$ with grid sizes described in **Table 3** and time steps of $\Delta t = 0.005$.

From examining the plot above we can see that lowering the H/L ratio results in a nondimensional force along the cavity lid with greater magnitude. This effect could arise from a number of potential causes. For one, the cavity with H/L = 0.5 has a greater proportion of the fluid interacting with the lid at any given time thus possibly explaining why a greater force was

experienced. Furthermore, the way in which the H/L ratio influences the actual properties of the flow (i.e. circulation, pressure gradient, etc.) may have much more to do with why the forces are so varied than we can confidently conclude from **Figure 11**.